Synthesis and structural characterisation of three dicyanamide complexes with Mn(II), Zn(II) and Cd(II): Supramolecular architectures stabilised by hydrogen bonding

Arpi Majumder [a], Guillaume Pilet [b], María Teresa Garland Rodriguez [c], Samiran Mitra [a,*]

[a] *Department of Chemistry, Jadavpur University, Kolkata 700 032, West Bengal, India*
[b] *Cristallographie et Ingénierie Moléculaire, Laboratoire des Multimatériaux et Interfaces – UMR 5615 Université Claude Bernard Lyon 1, Bât. Jules Raulin 43 Bd du 11 Novembre 1918, 69622 Villeurbanne Cedex, France*
[c] *Cimat, Laboratorio de Cristalografía, Universidad de Chile, Av. Blanco Encalada 2008, Santiago, Chile*

Abstract

Three new dicyanamido $[N(CN)_2]^-$ (dca) compounds of the formula $[Mn(ac)(tptz)(dca)(H_2O)]\cdot(H_2O)_2$ (**1**), $[Zn(tptz)(dca)_2]\cdot(H_2O)_2$ (**2**) and $[Cd_2(tptz)_2(dca)_2(H_2O)_2]\cdot(ClO_4)_2$ (**3**), (where ac = acetate anion and tptz = 2,4,6-tris(2-pyridyl)-1,3,5-triazine) have been synthesised. X-ray diffraction analysis revealed that the manganese atom in **1** is seven-coordinated with a pentagonal-bipyramidal environment, in **2** zinc is penta-coordinated square pyramidal and in **3** the cadmium atom is six-coordinated octahedral. dca is found to act as an end-to-end bridging ligand in the dimer **3**, whereas in **1** and **2** it acts as a monodentate terminal ligand. All the complexes exhibit supramolecular architectures by hydrogen bonding interactions involving lattice water (for **1** and **2**) or coordinated water molecules (for **3**).

Keywords: Structures; Dicyanamide; Pentagonal bipyramidal Mn(II); Square pyramidal Zn(II); Octahedral Cd(II); Hydrogen bonding interactions; Supramolecular architectures

1. Introduction

Supramolecular interactions are important in several fields of contemporary synthetic inorganic chemistry. Supramolecular structures are of great interest due to their structural characteristics, such as manifold coordination modes, intriguing architecture, and porosity, and also due to their physicochemical characteristics and potential applications as functional materials [1]. With the recent development of self-assembly supramolecular chemistry, it is possible to rationally design and synthesise supramolecular architectures based on covalent or supramolecular contacts [1b]. Supramolecules are often self-assembled systems by means of a variety of interactions which may interplay. In crystal engineering, synergistic effects between intermolecular non-covalent interactions are of great importance and must be regarded as a single interrelated entity [2]. The successful creation of higher-dimensional supramolecular architectures can be accomplished by employing coordination bonds, hydrogen bonds, aromatic π–π stacking interactions, etc. Recently, dicyanamide (dca) has been widely used as a building block in both supramolecular chemistry and crystal engineering [3]. The first report on coordination compounds with the pseudohalide dicyanamide anion $(N(CN)_2^-)$ was published by Madelung and Kern in 1922 and its coordinating ability towards 3d transition metal ions was explored by Köhler and coworkers in the 1960s and 1980s [4]. This pseudohalide ligand exhibits several coordination modes (Scheme 1) that account for its high versatility in the formation of intermetallic connections: monodentate bonding through a nitrile

* Corresponding author. Tel.: +91 33 26682017.
E-mail address: smitra_2002@yahoo.com (S. Mitra).

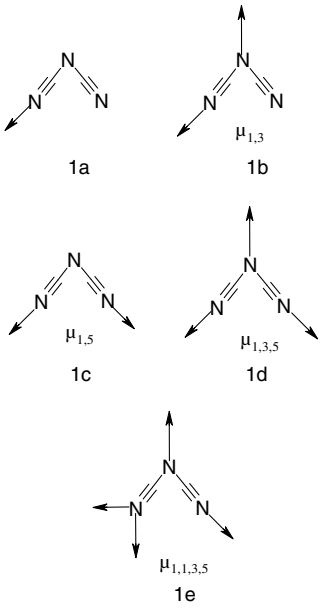

Scheme 1.

nitrogen, bidentate mode through two nitrile nitrogen atoms with end-to-end bridging, tris–monodentate bridging of three metal atoms, as well as an unusual μ-4 coordination where one nitrile nitrogen binds to two metal atoms. The coordination properties thus allow for the preparation of compounds with a large variety of architectures: mononuclear, dinuclear, as well as one-, two- and three-dimensional (nD, $n = 1$–3) networks [5] and therefore both its homo- and heteroleptic complexes have rich topologies and excellent magnetic properties [6]. A series of binary compounds of the general formula $[M^{II}(dca)_2]$, with a 3D rutile type structure, have gained much interest as several of these have been shown to be ferromagnetic (Co, $T_c = 9$ K; Ni, $T_c = 20$ K; Fe, $T_c = 19$ K), antiferromagnetic (Cr, $T_N = 47$ K; Mn, $T_N = 16$ K; Fe, $T_N = 19$ K) and paramagnetic [3]. Introduction of auxiliary ligands into the M^{II}–dca system has allowed the syntheses of several ternary systems, $[M^{II}L_x(dca)_y]$ (L = organic ligand, $x = 1$ or 2, $y = 1$ or 2), with a wide variety of topologies [7]. Coordination compounds with extended networks have been widely reported exhibiting different combinations of metallic cations, dipyridyl-type organic ligands and dca ligands [8]. A literature survey reveals the fact that dca-complexes in combination with 2,4,6-tris(2-pyridyl)-1,3,5-triazine (tptz) are rare. We have chosen tptz for its flexible coordination sites [9]. We have recently reported some novel observations utilising dca in the synthesis of chain structures with single, symmetrical, $\mu_{1,5}$-dca bridged Cu(II) and Ni(II) polymers [10]. In the present work, we describe the syntheses and crystal structures of three new supramolecular frameworks with dca and the auxiliary ligand, 2,4,6-tris(2-pyridyl)-1,3,5-triazine (tptz): $[Mn(ac)(tptz)(dca)(H_2O)] \cdot (H_2O)_2$ (**1**) (where ac = acetate anion), $[Zn(tptz)(dca)_2] \cdot (H_2O)_2$ (**2**) and $[Cd_2(tptz)_2(dca)_2(H_2O)_2] \cdot (ClO_4)_2$ (**3**). To date, a number of higher-dimensional architectures of different transition metals have been reported using dca as a bridging ligand, but the number of dinuclear compounds with bridging dca, are scarce [11]. To the best of our knowledge, this is the first dinuclear complex of Cd(II) using dca as a bridging ligand.

2. Experimental

2.1. Physical techniques

The infrared spectra of the complexes were recorded on a Perkin–Elmer RX 1 FT-IR spectrometer with a KBr disc. The electronic spectrum of **1** was recorded on a Perkin–Elmer Lambda 40 (UV–Vis) spectrophotometer in methanol. Elemental analyses were carried out using a Perkin–Elmer 2400 II elemental analyser. The electrochemical study was performed on a CH 600A cyclic voltammeter instrument for complex **1** in dimethylformamide solvent and using tetrabutylammonium perchlorate as the supporting electrolyte. The magnetic susceptibility was measured on a powder sample in a vibrating sample magnetometer for **1** using mercury(tetrathiocyanato)cobaltate as the standard.

2.2. Materials

All the chemicals and solvents used for the syntheses were of reagent grade. Manganese acetate tetrahydrate, zinc nitrate hexahydrate, cadmium perchlorate hydrate (Merck), 2,4,6-tris(2-pyridyl)-1,3,5-triazine (Aldrich) and sodium dicyanamide ($NaN(CN)_2$) (Fluka) were used as received. *Caution*! Although no problems were encountered in this work, perchlorate salts are potentially explosive. They should be prepared in small quantities and handled with care.

2.3. Synthesis

2.3.1. Synthesis of $[Mn(ac)(tptz)(dca)(H_2O)] \cdot (H_2O)_2$ (**1**)

Complex **1** was synthesised by adding 1 mmol (0.312 g) of tptz to a solution of 1 mmol (0.246 g) of manganese acetate tetrahydrate in 10 ml of methanol, followed by the dropwise addition of 1 mmol (0.089 g) of sodium dicyanamide dissolved in the minimum quantity of water. The resulting clear yellow solution was filtered off and left to stand in air. After 3 days, yellow needles of **1** were obtained that were suitable for X-ray determination. Yield: 0.41 g (74.6%). *Anal.* Calc. for $C_{22}H_{21}MnN_9O_5$: C, 48.31; H, 3.84; N, 23.06. Found: C, 48.25; H, 3.79; N, 22.97%.

2.3.2. Synthesis of $[Zn(tptz)(dca)_2] \cdot (H_2O)_2$ (**2**)

Crystals of complex **2** were separated as a pale yellow crystalline solid by adding 1 mmol (0.089 g) aqueous solution of sodium dicyanamide to a methanolic solution containing a mixture of zinc nitrate hexahydrate (1 mmol, 0.297 g) and tptz (0.312 g, 1 mmol). Yield: 0.39 g (72%).

Anal. Calc. for $C_{22}H_{16}N_{12}ZnO_2$: C, 48.36; H, 2.93; N, 30.77. Found: C, 48.32; H, 2.87; N, 30.71%.

2.3.3. Synthesis of $[Cd_2(tptz)_2(dca)_2(H_2O)_2]\cdot(ClO_4)_2$ (**3**)

Complex **3** was obtained as pale yellow hexagonal crystals by the reaction of 20 ml methanolic solution containing cadmium perchlorate hydrate (0.311 g, 1 mmol) and tptz (0.312 g, 1 mmol) with 10 ml aqueous of sodium dicyanamide (0.089 g, 1 mmol). Yield: 0.46 g (75%). *Anal.* Calc. for $C_{20}H_{14}CdClN_9O_5$: C, 39.32; H, 2.30; N, 20.64. Found: C, 39.23; H, 2.26; N, 20.51%.

2.4. X-ray crystallography

Experimental details for **1** and **3** are given in Table 1. The data processing was performed by the Kappa CCD analysis software [12] and the lattice constants were refined by least-square refinement. No absorption correction was applied to the data sets. The unit-cell parameters, crystal system, space group and refinement details are summarised in Table 1. The structures were solved by direct methods (SIR97 program [13]) combined with Fourier difference syntheses and refined against F using reflections with $[I/\sigma(I) > 3]$ (CRYSTALS program [14]). All non-hydrogen atoms were successfully refined anisotropically.

Intensity data for **2** were collected on a Bruker SMART APEX diffractometer, equipped with a CCD area detector and graphite monochromated Mo-Kα radiation ($\lambda =$ 0.71073 Å), controlled by a Pentium-based PC running the SMART software package [15]. Single crystals were mounted and measured at room temperature. All data were corrected for Lorentz and polarization effects. Semi-empirical absorption corrections were applied using the SADABS program [16]. Both data processing programs were integrated with the Bruker SAINTPLUS program [17]. The structure was solved by the Patterson method, completed by difference Fourier techniques and refined by full-matrix least-squares on F^2 (SHELXL/97) [18] with initial isotropic, but subsequently anisotropic thermal parameters. Hydrogen atoms were included in calculated positions and refined riding on carbon atoms with free isotropic displacement parameters. The hydrogen atoms of the two water molecules were located from the difference Fourier map, and their positions were refined with a restrained O–H = 0.9 Å distance [18]. Further details are given in Table 1.

3. Results and discussion

3.1. Description of the crystal structures

3.1.1. $[Mn(ac)(tptz)(dca)(H_2O)]\cdot(H_2O)_2$ (**1**)

The molecular structure of **1** is shown in Fig. 1. Selected bond distances and bond angles are presented in Table 2. Each manganese atom is hepta-coordinated, with a coordination polyhedron close to a pentagonal bipyramid. Hepta-coordination is achieved by means of three N atoms belonging to the tptz ligand (N10, N21 and N33) and two

Table 1
Crystallographic data of complexes **1**–**3**

	1	**2**	**3**
Chemical formula	$C_{22}H_{21}MnN_9O_5$	$C_{22}H_{16}N_{12}ZnO_2$	$C_{20}H_{14}CdCl_1N_9O_5$
Formula weight	546.40	545.84	608.24
Crystal system	monoclinic	triclinic	triclinic
Temperature (K)	293	295	293
Space group	$C2/c$	$P\bar{1}$	$P\bar{1}$
a (Å)	14.668(5)	9.250(9)	7.956(5)
b (Å)	13.394(3)	10.558(10)	10.751(5)
c (Å)	26.821(9)	13.354(13)	14.043(5)
α (°)	90	110.758(10)	72.295(5)
β (°)	99.613(1)	98.480(2)	80.237(5)
γ (°)	90	100.659(2)	83.170(5)
V (Å^3)	5195.7(3)	1166.0(2)	1125(1)
Z	8	2	2
Reflections collected	10988	8572	6697
Independent reflections	5908	5035	5493
R_{int}	0.029	0.018	0.02
Density (calculated) (Mg m^{-3})	1.361	1.555	1.796
Absorption coefficient (mm^{-1})	0.555	1.101	1.143
$F(000)$	2248	548	604
Crystal size (mm)	$0.01\times0.01\times0.06$	$0.42\times0.39\times0.27$	$0.01\times0.01\times0.09$
θ Range for data collection	1.5–27.6	1.7–28.0	1.5–30.2
Number of restraints	9	6	3
R indices (all data)	$R_1 = 0.1179$	$R_1 = 0.0493$	$R_1 = 0.0887$
	$wR_2 = 0.1148$	$wR_2 = 0.1076$	$wR_2 = 0.0951$
Final R indices $[I > 3\sigma(I)$ for **1** and **3**] and $[I > 2\sigma(I)$ for **2**]	$R_1 = 0.0498$	$R_1 = 0.0409$	$R_1 = 0.0480$
	$wR_2 = 0.0595$	$wR_2 = 0.1026$	$wR_2 = 0.0527$
Largest difference in peak and hole (e Å^3)	0.57, −0.52	0.52, −0.35	0.65, −0.61

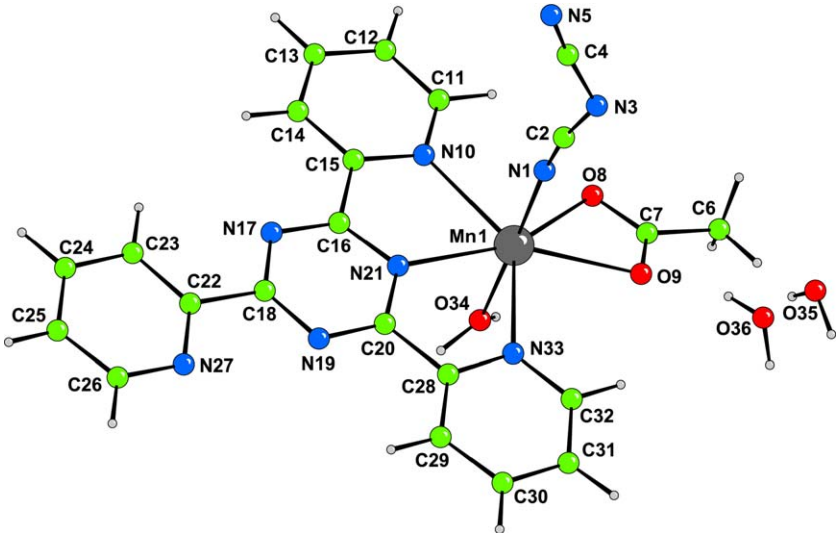

Fig. 1. Coordination environment of the metal in complex **1** with the atom numbering scheme.

Table 2
Selected bond distances (Å) and bond angles (°) for complex **1**

Mn1–O8	2.291(3)	C13–C14	1.387(6)
Mn1–O9	2.347(3)	C16–N17	1.324(5)
Mn1–O34	2.137(3)	C18–N19	1.331(5)
Mn1–N1	2.184(5)	C22–C23	1.387(6)
Mn1–N10	2.415(4)	C25–C26	1.369(7)
Mn1–N21	2.292(3)	C28–C29	1.370(5)
Mn1–N33	2.390(3)	C31–C32	1.369(6)
N1–C2	1.094(6)	C11–C12	1.380(6)
N3–C2	1.279(8)	C14–C15	1.375(6)
N3–C4	1.290(9)	C23–C24	1.389(6)
N5–C4	1.097(9)	C26–N27	1.341(6)
C15–C16	1.488(5)	C29–C30	1.392(7)
C18–C22	1.497(6)	C32–N33	1.340(5)
C20–C28	1.476(5)	C12–C13	1.366(7)
O8–Mn1–O9	55.76(9)	O34–Mn1–N1	177.48(13)
O8–Mn1–O34	85.66(10)	O34–Mn1–N10	90.23(10)
O8–Mn1–N1	96.82(14)	O34–Mn1–N21	85.82(11)
O8–Mn1–N10	85.95(10)	O34–Mn1–N33	84.76(10)
O8–Mn1–N21	152.76(10)	N1–Mn1N10	89.52(13)
O8–Mn1–N33	136.13(10)	N1–Mn1–N21	91.77(13)
O9–Mn1–O34	94.79(10)	N1–Mn1–N33	93.71(13)
O9–Mn1–N1	86.98(13)	N10–Mn1–N21	68.26(11)
O9–Mn1–N10	140.71(10)	N10–Mn1–N33	136.71(11)
O9–Mn1–N21	150.92(10)	N21–Mn1–N33	68.50(10)
O9–Mn1–N33	82.58(9)		

oxygen atoms from the bidentate acetato ligand (O8 and O9), which determine the equatorial plane and finally the nitrogen N1 atom from the terminal dicyanamido ligand and a water molecule (O34) are in a *trans* disposition (yielding N1–Mn1–O34 as the *trans-axial* angle 177.48(13)°).

The shorter bond lengths, 2.184(5) and 2.137(3) Å, correspond to the axial positions occupied by the terminal monodentate dca ligand, Mn1–N1 and water molecule Mn1–O34, respectively, whereas the equatorial sites show similar bond lengths in the 2.291(3)–2.415(4) Å range which are more or less comparable to similar systems [9,19]. The deviation from ideal pentagonal-bipyramidal geometry is indicated by the difference in the basal angles which vary from 85.95(10)° to 55.76(9)°. The source of distortion primarily comes from the bites taken by the ligand, smaller than the ideal value of 72°, because of the constraint imposed in the five-membered chelate rings. Three kinds of bond angles may be found in the equatorial plane: the lower of 55.76(9)° corresponds to the bidentate acetate ligand O8–Mn1–O9 bond angle, two intermediate ones of 68.50(10)° and 68.26(11)° corresponding to the N(tptz)–Mn1–N(tptz) bond angles and two greater O(acetate)–Mn1–N(tptz) bond angles of 85.95(10)° and 82.58(9)°. These values are consistent with those found for related complexes [20]. The bond distance of Mn(II) to the middle nitrogen N21 is significantly shorter than the Mn1–N10 and Mn1–N33 distances, which is usually observed in tptz-type ligands [19]. The tptz ligand is almost planar; the angles between the central triazine ring and the attached pyridyl rings are 2.5(1)°, 2.1(1)° and 3.5(1)° which are in accordance with the values reported in the literature in related systems [9,21] and the tptz plane is inclined by an angle of 15.7(1)° to the bidentate acetate plane. In tptz, the $C(sp^2)$–$C(sp^2)$ distances within the ring are normal (1.45 Å) and the exterior bonds (C16–C15, 1.48(5) Å; C20–C28, 1.47(5) Å; C18–C22, 1.49(6) Å) are also normal. The manganese atom is 0.071(1) Å out of the basal pentagonal plane. The deviations of the atoms N10, N21, N33, O8 and O9 from the mean basal plane are 0.097(3), −0.003(3), −0.092(3), 0.195(3) and 0.194(3) Å, respectively. The dihedral angles between the equatorial plane and the plane of the tptz and dca groups are 3.11(5)° and 86.6(2)°, respectively.

The structure also contains uncoordinated water molecules in the lattice. Both hydrogen atoms of the coordinated water molecule (O34) are involved in making hydrogen bonds with (i) the oxygen atom of an uncoordinated water molecule (O35) and with (ii) the oxygen atom (O8) of the counter anion ($CH_3CO_2^-$) which belongs to a

Table 3
Hydrogen bonds for **1** (Å and °)

D–H···A	d(D–H)	d(H···A)	d(D···A)	⟨(DHA)⟩
O34–H341···O8^{i}	0.89(2)	1.80(3)	2.678(4)	173(4)
O34–H342···O35^{ii}	0.89(3)	1.82(3)	2.693(4)	170(3)
O35–H351···O36	0.89(3)	1.84(3)	2.720(6)	168(2)
O35–H352···N27^{iii}	0.88(3)	2.06(3)	2.906(6)	160(3)
O36–H361···N5^{iv}	0.90(3)	2.01(3)	2.875(8)	160(3)
O36–H362···O9	0.89(3)	1.93(3)	2.791(6)	166(3)
C11–H101···O8	1.0100	2.5900	3.243(5)	122.00
C23–H221···N5^{v}	1.0200	2.5900	3.504(9)	149.00
C29–H281···O35^{vi}	1.0100	2.4700	3.471(6)	172.00
C32–H284···O9	1.0100	2.4100	3.103(5)	125.00

Symmetry transformations used to generate equivalent atoms: (i) $2-x, y, 1/2-z$; (ii) $1/2+x, 1/2+y, z$; (iii) $3/2-x, -1/2-y, -z$; (iv) $1/2+x, -1/2+y, z$; (v) $1/2+x, 1/2+y, z$; (vi) $3/2-x, -1/2-y, -z$.

neighbouring manganese-complex. Thus, infinite chains are formed. The second oxygen atom (O9) of the $CH_3CO_2^-$ anion makes a hydrogen bond with one of the hydrogen atoms of the other lattice water molecule (O36). O36 is also connected to N5 (the terminal nitrogen atom of the $N(CN)_2^-$ ligand) and is further involved in hydrogen bonding interactions to the other neighbouring terminal nitrogen atom and thus connects the 1D chains together to form 2D sheets which lie in the [1 0 0] plane. O35 is connected via hydrogen bonds to O36 and to N27 (nitrogen atoms belonging to the external ring of the tptz ligand connected to another manganese-complex), connecting the sheets together to form a 3D supramolecular network. Due to the presence and the number of uncoordinated water molecules inside this structure, many hydrogen bonds are formed connecting isolated complexes together and thus the structure can be assumed to be a pseudo 3D network (Table 3, Fig. 2). This hydrogen bonding network is reinforced by two types of weak C–H···O interactions (Table 3). This weak hydrogen bonding is possibly a contributing factor in the supramolecular assembly and stabilisation of the lattice, however, the strong O–H···O interactions are obviously the dominant intermolecular interactions. The significant π–π stacking distance between the two parallel planar rings of the tptz ligand is 3.76(1) Å. This distance is very similar to other π–π stacked systems [22].

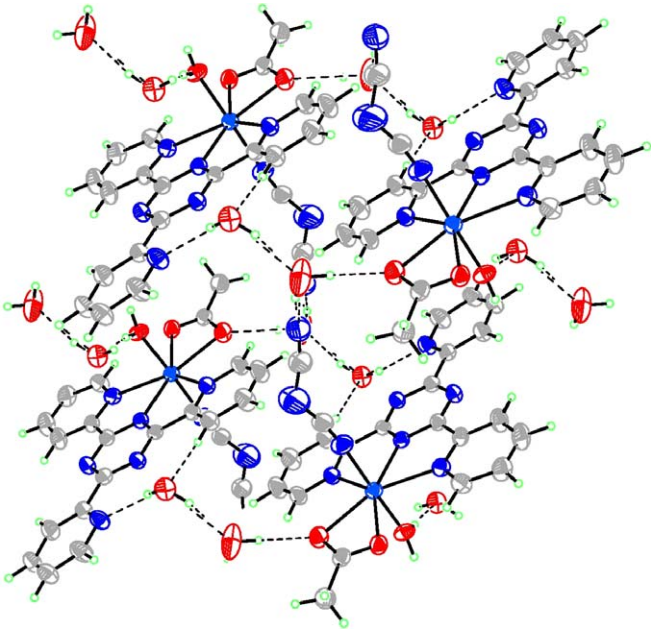

Fig. 2. Hydrogen bonds building 3D networks in **1**.

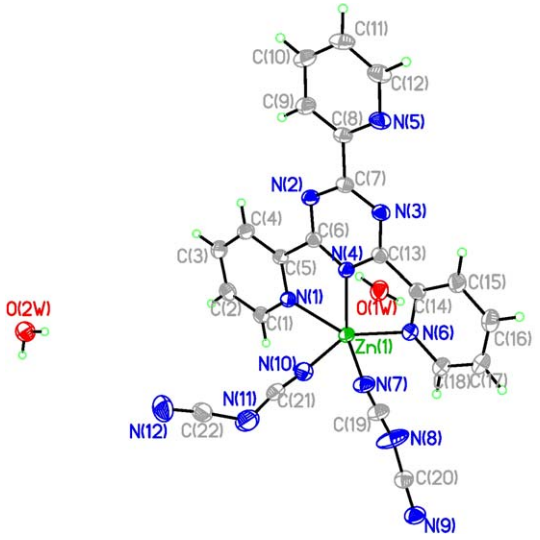

Fig. 3. Local coordination environment of the metal in complex **2** with the atom numbering scheme.

3.1.2. *[Zn(tptz)(dca)$_2$]·(H$_2$O)$_2$ (**2**)*

The structure of **2** consists of the neutral mononuclear unit, $[Zn(tptz)(dca)_2]\cdot(H_2O)_2$ (Fig. 3), in which the three tptz nitrogen atoms and a terminal dca nitrogen bind to zinc in equatorial positions (Zn1–N1, 2.216(2) Å; Zn1–N4, 2.077(2) Å; Zn1–N6, 2.225(2) Å and Zn1–N7, 1.974(3) Å), and another terminal dca nitrogen resides in an apical position (Zn–N10, 2.064(2) Å). Considering these bonds, the zinc coordination geometry may be described as distorted square pyramidal, the trigonality parameter τ being 0.21 [23].

Selected bond distances and bond angles are summarised in Table 4. The Zn–pyridyl bond distances are comparable and the values are similar to those found in similar systems [24]. The deviation from the ideal square pyramid is indicated by the difference in *cisoid* (63.53(8)–110.29(10)°) and *transoid* angles (147.62(7)–160.22(11)°). The source of distortion primarily comes from the bites taken by the ligand; the bite angles N1–Cd1–N4 and N4–Cd1–N6 are 74.21(7)° and 73.53(8)°, respectively, significantly smaller than the ideal value of 90°. The deviations of the atoms N1, N4, N6 and N7 from the mean basal plane are −0.0850, +0.1121, −0.0910 and 0.0638 Å, respectively, and the zinc atom is displaced by 1.1202 Å from the plane towards the apical dca. The dihedral angles between the equatorial plane and the plane of the tptz and two dca groups are 8.5°, 62.7° (apical) and 58.4°, respectively. The

Table 4
Selected bond distances (Å) and bond angles (°) for complex **2**

Zn1–N1	2.216(2)	C7–C8	1.482(4)
Zn1–N4	2.077(2)	C1–C2	1.370(4)
Zn1–N6	2.225(2)	C2–C3	1.395(4)
Zn1–N7	1.974(3)	C3–C4	1.381(4)
Zn1–N10	2.064(2)	C4–C5	1.380(3)
N7–C19	1.143(4)	C8–C9	1.375(4)
N8–C20	1.300(3)	C9–C10	1.376(4)
N8–C19	1.277(4)	C10–C11	1.377(5)
N9–C20	1.138(3)	C11–C12	1.368(4)
N10–C21	1.126(4)	C13–C14	1.480(3)
N11–C22	1.284(4)	C14–C15	1.379(4)
N11–C21	1.287(4)	C15–C16	1.386(4)
N12–C22	1.120(5)	C16–C17	1.380(5)
C5–C6	1.483(3)	C17–C18	1.372(5)
N1–Zn1–N4	74.21(7)	N4–Zn1–N7	160.22(11)
N1–Zn1–N6	147.62(7)	N4–Zn1–N10	101.08(9)
N1–Zn1–N7	110.29(10)	N6–Zn1–N7	99.30(10)
N1–Zn1–N10	90.83(9)	N6–Zn1–N10	97.92(10)
N4–Zn1–N6	73.53(8)	N7–Zn1–N10	98.14(11)

pyridyl rings of tptz are planar and the angles between the central triazine ring and the attached pyridyl rings are 1.8° (Py–N1), 2.7° (Py–N5) and 2.4° (Py–N6). The tptz group acts as a tridentate ligand through its three nitrogen atoms, the zinc to triazine-nitrogen (N4) bond being significantly shorter than the two zinc to pyridyl-nitrogen ones (Zn1–N1 and Zn1–N6 distances), a pattern usually observed in this type of three point attachment of tptz-type ligands [25]. The average $C(sp^2)$–$C(sp^2)$ bond lengths in the tptz ligand within the ring are normal and the exterior bonds (C5–C6, 1.483(3) Å; C7–C8, 1.482(4) Å; C13–C14, 1.480(3) Å) are also in agreement with those reported previously [26] and with complexes **1** and **3** also.

There are extensive arrays of hydrogen bonding interactions involving the dicyanamide, tptz moieties and lattice water molecules yielding a 1D supramolecular chains-like architecture (Fig. 4, Table 5). The two lattice water molecules with their centrosymmetric homologous are linked by strong hydrogen bonds, giving rise to quadrilateral frameworks (O1W–H2W···O2W = 2.864(3) Å and O2W–H4W···O1W = 2.854(3) Å). The four remaining hydrogen atoms bind, respectively, to two terminal nitrogen atoms of $N(CN)_2^-$ ligands and two pyridyl nitrogen atoms (belonging to the external ring of the tptz ligand) of the neighbouring zinc complex (Fig. 4 and Table 5). The resulting supramolecular network thus can be described as layers of complexes with the aromatic ligands lying parallel to (1 0 1) planes linked by hydrogen bonds provided by the water molecules. There are also weak π–π interactions between tptz ligands (closest non-hydrogen contact is 3.644 (2) Å).

3.1.3. $[Cd_2(tptz)_2(dca)_2(H_2O)_2]\cdot(ClO_4)_2$ (**3**)

A perspective view of complex **3** with the atom numbering scheme is shown in Fig. 5. Selected bond distances and bond angles are summarised in Table 6. Two dca groups bridge the metal atoms in a symmetric end-to-end fashion.

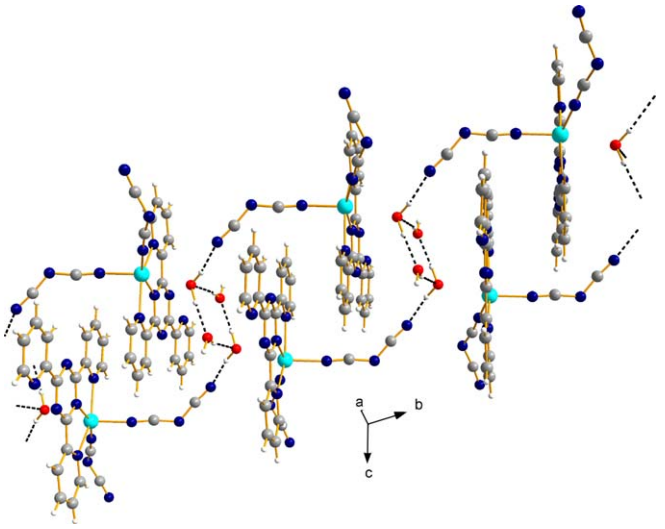

Fig. 4. Perspective view of **2** showing 1D-layers formed by the hydrogen bond interaction in the [0 1 0] plane. Hydrogen atoms are omitted for clarity.

Table 5
Hydrogen bonds for **2** (Å and °)

D–H···A	*d*(D–H)	*d*(H···A)	*d*(D···A)	⟨(DHA)⟩
O1W–H1W···N12^{i}	0.88(4)	1.96(4)	2.836(4)	169(4)
O1W–H2W···O2W^{ii}	0.99(4)	1.88(4)	2.864(3)	172(3)
O2W–H3W···N3^{iii}	0.90(4)	2.62(4)	3.439(3)	152(4)
O2W–H3W···N5^{iii}	0.90(4)	2.21(5)	2.944(3)	138(4)
O2W–H4W···O1W^{iv}	0.87(4)	2.01(4)	2.854(3)	165(4)
C3–H3···N9^{v}	0.93	2.53	3.445(4)	167.00
C9–H9···N2	0.93	2.48	2.796(3)	100.00

Symmetry transformations used to generate equivalent atoms: (i) x, $1+y$, z; (ii) $-x$, $1-y$, $2-z$; (iii) $1-x$, $1-y$, $2-z$; (iv) x, $-1+y$, z; (v) x, y, $1+z$.

Complex **3** is an unusual dinuclear entity bridged by dca. One nitrogen from triazine and two from pyridyl moieties along with the two dca anions and one water molecule form the distorted octahedral geometry around each Cd(II). Three nitrogen atoms (N18, N1 and N12) from the tptz ligand and one bridging dca (N25) form the mean equatorial base, while O35 from water and N29 from another bridging dicyanamide occupy the axial positions.

The bond lengths are in accordance with those observed in the literature [27]. The deviation from ideal octahedral geometry is indicated by the difference in *cisoid* (67.97(15)–122.9(2)°) and *transoid* angles (136.84(14)–172.75(19)°). The deviations of the atoms N1, N12, N18 and N25 from the mean basal plane are 0.073(4), −0.070(5), −0.057(4) and 0.076(6) Å. The source of distortion primarily comes from the bites taken by the ligand; the bite angles N18–Cd1–N1 and N1–Cd1–N12 are 67.97(15)° and 68.87(15)°, respectively, significantly smaller than the ideal value of 90°. The bond distance of Cd(II) to the middle nitrogen N1 (2.330(4) Å) is significantly shorter than the Cd1–N18 (2.426(4) Å) and Cd1–N12 (2.378(6) Å) distances, a pattern observed for complexes **1**–**3**, and the values are comparable for these types of bonds [28]. The

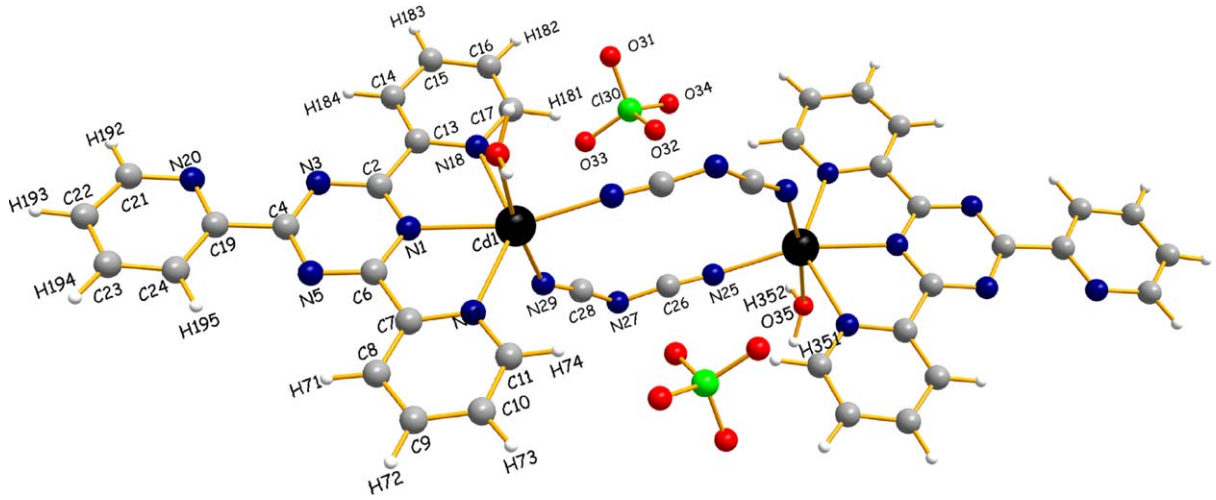

Fig. 5. Perspective view of the dinuclear unit in **3** showing the atom numbering scheme.

Table 6
Selected bond distances (Å) and bond angles (°) for complex **3**

Cd1–O35	2.365(5)	C21–C22	1.391(9)
Cd1–N1	2.330(4)	C22–C23	1.359(9)
Cd1–N12	2.378(6)	C23–C24	1.390(9)
Cd1–N18	2.426(4)	C19–C24	1.389(8)
Cd1–N25	2.199(7)	C13–C14	1.382(8)
Cd1–N29	2.287(6)	C14–C15	1.395(9)
N25–C26	1.130(10)	C15–C16	1.374(9)
N27–C28	1.275(10)	C16–C17	1.370(8)
N27–C26	1.260(10)	C13–C14	1.382(8)
N29–C28	1.133(9)	C7–C8	1.378(9)
C6–C7	1.486(7)	C8–C9	1.375(10)
C2–C13	1.483(7)	C9–C10	1.380(11)
C4–C19	1.495(7)	C10–C11	1.385(11)
O35–Cd1–N1	84.35(16)	N1–Cd1–N29	102.32(17)
O35–Cd1–N12	90.94(18)	N12–Cd1–N18	136.84(14)
O35–Cd1–N18	85.28(16)	N12–Cd1–N25	122.9(2)
O35–Cd1–N25	84.5(2)	N12–Cd1–N29	94.10(18)
O35–Cd1–N29	172.75(19)	N18–Cd1–N25	99.6(2)
N1–Cd1–N12	68.87(15)	N18–Cd1–N29	94.55(17)
N1–Cd1–N18	67.97(15)	N25–Cd1–N29	88.4(2)
N1–Cd1–N25	163.9(2)		

Table 7
Hydrogen bonds for **3** (Å and °)

D–H···A	*d*(D–H)	*d*(H···A)	*d*(D···A)	⟨(DHA)⟩
N27–H272···N27^{i}	1.00	2.61	3.13(8)	112.00
O35–H351···O34^{ii}	0.95(6)	1.89(6)	2.797(10)	160(4)
O35–H352···N20^{iii}	0.94(4)	2.07(5)	2.954(7)	155(4)
C8–H71···O31^{iv}	1.0200	2.4700	3.383(11)	149.00
C11–H74···O34	1.0200	2.3400	3.249(11)	148.00
C16–H182···O31^{v}	1.0200	2.4400	3.190(12)	130.00
C15–H183···O33^{vi}	1.0200	2.4900	3.464(11)	161.00
C14–H184···O35^{iii}	1.0200	2.4800	3.444(8)	158.00

Symmetry transformations used to generate equivalent atoms: (i) $2-x$, $-y$, $2-z$; (ii) $1-x$, $1-y$, $2-z$; (iii) $1-x$, $1-y$, $1-z$; (iv) $-x$, $1-y$, $2-z$; (v) $1-x$, $-y$, $2-z$; (vi) x, y, $-1+z$.

Cd1–N(dca) distances vary from 2.199(7) to 2.287(6) Å and Cd1–O(water) is 2.365(5) Å. In the ligand tptz, the C(sp^2)–C(sp^2) distances within the ring are normal (in the range 1.272(10)–1.486(7) Å) and the exterior bond distances (C6–C7, 1.486(7) Å; C2–C13, 1.483(7) Å; C4–C19, 1.495(7) Å) are also normal. The tptz ligands do not deviate much from planarity [24,29]; the three pyridyl rings are twisted with respect to the central triazine ring by angles of 0.8(1)°, 4.5(1)° and 4.6(1)°, with the non-coordinating ring displaying the highest degree of twisting. The cadmium···cadmium separation within the dinuclear unit is 7.537(5) Å, and the shortest inter-dimer cadmium···cadmium distance is 7.713(1) Å. Each dimer is connected to each other via hydrogen bonding interactions, building infinite neutral chains running along the following vector: [0.08; −0.47; 0.87]. The structural cohesion between these chains is then assumed by coulombic interactions. Both the hydrogen atoms of O35 are involved in hydrogen bonding interactions: (i) with the oxygen atom of the ClO_4^- counter anion; (ii) with one nitrogen atom (N20) of the external pyridyl ring of the tptz ligand belonging to the neighbouring cadmium. The later hydrogen bond allows the connection between dimers to form infinite chains. These 1D chains are further connected into supramolecular 2D sheets along the *bc*-plane (Table 7, Fig. 6). There exist weak π–π interactions between the tptz ligands (closest non-hydrogen contact is equal to 3.77(2) Å). The directed H-bond, which gives this complex an overall 2D structure, may be responsible for the stabilisation of the coordinated dinuclear form.

3.2. Infrared spectra

Complexes **1**–**3** exhibit strong absorptions in the region 2325–2155 cm^{-1} that correspond to $\nu_{C\equiv N}$ modes for dca groups, attributed to $\nu_{as} + \nu_s(C\equiv N)$ combination modes, $\nu_{as}(C\equiv N)$ and $\nu_s(C\equiv N)$. The shift towards higher wave numbers for the peaks of dca in **1**–**3** when compared to those of free dicyanamide is consistent with the coordination of dca in the complexes. These three bands appear at 2293, 2239, 2177 cm^{-1} for complex **1**, at 2299, 2237, 2178 cm^{-1} for complex **2**, and at 2312, 2245, 2183 cm^{-1}

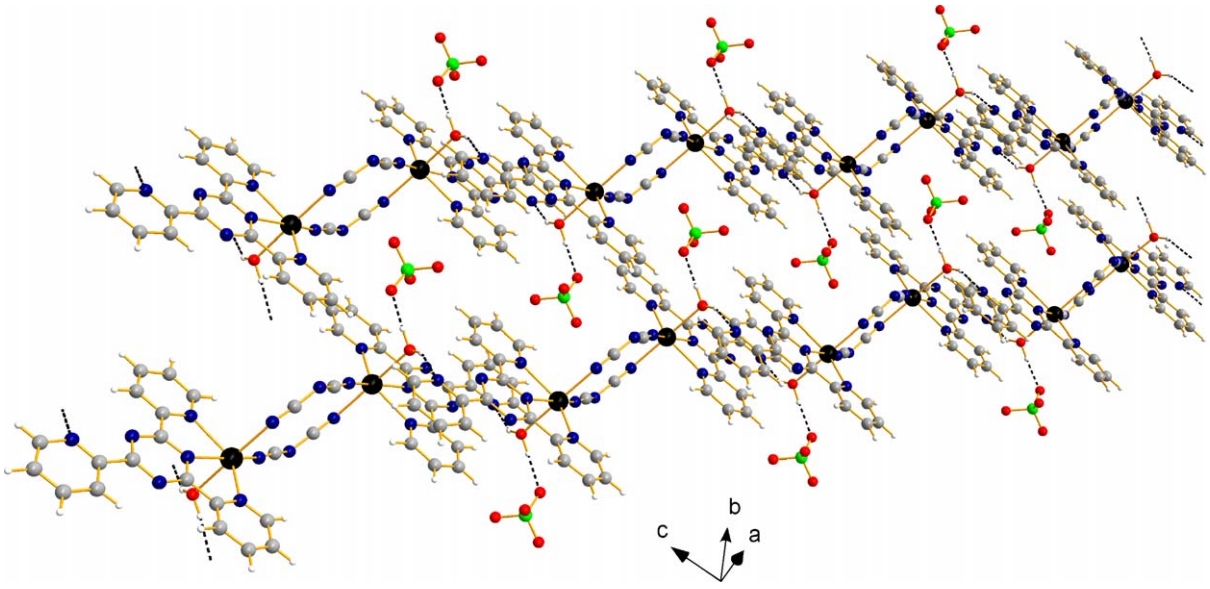

Fig. 6. 3D-supramolecular architecture formed by the hydrogen bonding interactions in **3**.

for complex **3** [1,5,11,30]. Bands dealing with the ν_{as}(C–N) stretching frequencies (1400–1300 cm^{-1} region) and the ν_s(C–N) stretch (950–900 cm^{-1} region) occur in all the spectra. Additionally, pyridyl ring breathing signals have been detected around 1050 cm^{-1} for these compounds. Complex **1** shows a broad signal at about 3400 cm^{-1} which corresponds to coordinated water and indicates the presence of hydrogen bonding [1a]. A strong and broad absorption at 3340 cm^{-1} (O–H stretching of water) in the infrared spectrum of **3** is due to the presence of coordinated water with hydrogen bonds [30b]. Strong bands at 1560 and 1520 cm^{-1} for **1**, 1564 and 1519 cm^{-1} for **2** and 1572 and 1524 cm^{-1} for **3** correspond to the coordinated tptz ligand. Peaks at 1625, 1593, 1530, 1479, 1461, 1443, 1369 and 973 cm^{-1} present in **1**–**3** can be assigned to the C=C and C=N ring stretching vibrations [19]. Peaks are also observed at 766 cm^{-1} (C–H stretching) and 586 cm^{-1} (pyridyl out-of-ring deformation) for all the three complexes [31]. The characteristic strong bands of carboxylate groups appeared at 1560 (for asymmetric stretching) and 1416 cm^{-1} (for symmetric stretching) [19,31]. The difference ($\Delta\nu = 144\ cm^{-1}$) between $\nu_{asym}(COO^-)$ and $\nu_{sym}(COO^-)$ bands suggests the presence of a chelating acetate group linked with the metal center for complex **1**. Broad intense bands at ca. 1100 cm^{-1} due to ClO_4^- show no splitting, indicating the absence of coordinated ClO_4^- in **1** [32].

3.3. Electronic spectrum

The electronic spectrum of **1** was recorded in dimethylformamide and showed two strong bands at about 240 and 265 nm which are clearly charge transfer in origin and an absorption band observed at 295 nm can be assigned to charge transfer from the coordinated ligand to Mn(II). The complex does not show any d–d transitions [33].

3.4. Electrochemical study

An electrochemical study of complex **1** was performed using dimethylformamide as solvent and tetrabutylammonium perchlorate as the supporting electrolyte at a scan rate of 50 mV s^{-1}. One irreversible reductive response at −1.05 V versus SCE was observed, which is attributed to a ligand-centered reduction. No oxidation response was found on the positive side of SCE.

3.5. Magnetic study

The effective magnetic moment at 20 °C for complex **1** is 5.98 BM, which is near to the spin-only value of the manganese(II) ion relative to mercury(tetrathiocyanato)cobaltate as the standard.

4. Conclusion

We have synthesised three dicyanamido complexes obtained from room temperature reactions. Complexes **1** and **2** are mononuclear and complex **3** is a dicyanamide-bridged dinuclear complex. To the best of our knowledge, complex **3** is the first example of a dicyanamide-bridged dinuclear cadmium(II) system. In fact, dca has a strong tendency to form polymeric complexes and that is why dinuclear dicyanamido-bridged complexes are rare in the literature. The difference in preferred coordination number between manganese (5–7), zinc (4–6) and cadmium (2–8) inspires significant differences in their respective structures. Here, the numerous hydrogen bonding interactions

involving the constituent materials enhance the stability of all the complexes and lead to the supramolecular architectures.

5. Supplementary material

Crystallographic data for the structural analysis have been deposited with the Cambridge Crystallographic Data Centre, CCDC Nos. 284526–284528 for **1**–**3**, respectively. Copies of this information may be obtained free of charge from The Director, 12 Union Road, Cambridge, CB2 1EZ, UK (fax: +44 1223 336 033; e-mail: deposit@ccdc.cam.ac.uk or http://www.ccdc.cam.ac.uk).

Acknowledgements

The research was supported by grant from DST, New Delhi, India. We thank Dr. Andrés Ibañez for the structural data analysis and the diagrams.

References

[1] (a) C.-B. Liu, M.-X. Yu, X.-J. Zheng, L.-P. Jin, S. Gao, S.-Z. Lu, Inorg. Chim. Acta 358 (2005) 2687;
(b) C.R. Peŕez, P.L. Luis, M.H. Molina, M.M. Laz, Fernando S. Delgado, P. Gili, M. Julve, Eur. J. Inorg. Chem. (2004) 3873.
[2] H. Casellas, C. Massera, P. Gamez, A.M.M. Lanfredi, Jan Reedijk, Eur. J. Inorg. Chem. (2005) 2902.
[3] W. Dong, Q.-L. Wang, Z.-Q. Liu, D.-Z. Liao, Z.-H. Jiang, S.-P. Yan, P. Cheng, Polyhedron 22 (2003) 3315.
[4] J. Carranza, C. Brennan, J. Sletten, F. Lloret, M. Julve, J. Chem. Soc., Dalton Trans. (2002) 3164.
[5] B. Vangdal, J. Carranza, F. Lloret, M. Julve, J. Sletten, J. Chem. Soc., Dalton Trans. (2002) 566.
[6] Y.-Q. Xu, J.-H. Luo, D.-Q. Yuan, Y. Xu, R. Cao, M.-C. Hong, J. Mol. Struct. (2003) 658.
[7] I. Riggio, G.A. van Albada, D.D. Ellis, A.L. Spek, J. Reedijk, Inorg. Chim. Acta 313 (2001) 120.
[8] S. Martín, M.G. Barandika, J.M. Ezpeleta, R. Cortés, J.I.R. de Larramendi, L. Lezama, T. Rojo, J. Chem. Soc., Dalton Trans. (2002) 4275.
[9] A. Majumder, C.R. Choudhury, S. Mitra, C. Marschner, J. Baumgartner, Z. Naturforsch. 60b (2005) 99.
[10] (a) R. Karmakar, C.R. Choudhury, D.L. Hughes, G.P.A. Yap, M.S. El Fallah, C. Desplanches, J.-P. Sutter, S. Mitra, Inorg. Chim. Acta 359 (2006) 1184;
(b) S. Sen, P. Talukder, S. Mitra, G. Rosair, G. Yap, V. Gramlich, J. Kim, T. Matsushita, C. Desplanches, J.-P. Sutter, Inorg. Chim. Acta 358 (2005) 4534.
[11] D. Ghoshal, H. Bialas, A. Escuer, M. Font-Bardía, T.K. Maji, J. Ribas, X. Solans, R. Vicente, E. Zangrando, N. Ray Chaudhuri, Eur. J. Inorg. Chem. (2003) 3929.
[12] Nonius COLLECT, DENZO, SCALEPACK, SORTAV: KappaCCD Program us B.V., Delft, The Netherlands, 1999.
[13] G. Cascarano, A. Altomare, C. Giacovazzo, A. Guagliardi, A.G.G. Moliterni, D. Siliqi, M.C. Burla, G. Polidori, M. Camalli, Acta Crystallogr., Sect. A 52 (1996) C-79.
[14] D.J. Watkin, C.K. Prout, J.R. Carruthers, P.W. Betteridge, CRYSTAL Issue 11, Chemical Crystallography Laboratory, Oxford, UK, 1999.
[15] Bruker, SMART-NT Version 5.629 Bruker AXS Inc., Madison, WI, USA, 2000.
[16] G.M. Sheldrick, SADABS, University of Göttingen, Germany, 1996.
[17] Bruker, SAINT-NT Version 6.45 Bruker AXS Inc., Madison, WI, USA, 2000.
[18] G.M. Sheldrick, SHELXTL/PC, Version 6.10 Bruker AXS Inc., Madison, WI, USA.
[19] A. Escuer, F.A. Mautner, Nuŕia Sanz, R. Vicente, Inorg. Chim. Acta 340 (2002) 163.
[20] (a) C.W. Chan, C.M. Che, S.M. Peng, Polyhedron 12 (1993) 2169;
(b) A. Claramunt, A. Escuer, F.A. Mautner, N. Sanz, R. Vicente, J. Chem. Soc., Dalton Trans. (2000) 2627;
(c) M.K. Kabir, M. Kawahara, H. Kumagai, K. Adachi, S. Kawata, T. Ishii, S. Kitagawa, Polyhedron 20 (2001) 1417;
(d) M.K. Kabir, M. Kawahara, K. Adachi, S. Kawata, T. Ishii, S. Kitagawa, Mol. Cryst. Liq. Cryst. 376 (2002) 65;
(e) Y.G. Yin, K.K. Cheung, W.T. Wong, Chem. J. Chin. Univ. 21 (2000) 5.
[21] J. Kim, S. Han, Acta Crystallogr., Sect. C 58 (2002) m521.
[22] C. Janiak, J. Chem. Soc., Dalton Trans. (2000) 3885.
[23] A.W. Addison, T.N. Rao, J. Reedijk, J.V. Rijn, G.C. Verschoor, J. Chem. Soc., Dalton Trans. (1984) 1349.
[24] P. Gamez, P. de Hoog, M. Lutz, W.L. Driessen, A.L. Spek, J. Reedijk, Polyhedron 22 (2003) 205.
[25] (a) M.A. Harvey, S. Baggio, R. Baggio, Acta Crystallogr., Sect. C 60 (2004) m498;
(b) F. Marandia, A.A. Soudia, A. Morsali, R. Kempe, Z. Anorg. Allg. Chem. 631 (2005) 3070.
[26] M. Harvey, S. Baggio, S. Russi, R. Baggio, Acta Crystallogr., Sect. C 59 (2003) m171.
[27] (a) J. Luo, M. Hong, J. Weng, Y. Zhao, R. Cao, Inorg. Chim. Acta 329 (2002) 59;
(b) O.V. Nesterova (Pryma), S.R. Petrusenko, V.N. Kokozay, B.W. Skelton, W. Linert, Inorg. Chem. Commun. 7 (2004) 450;
(c) J.-H. Luo, M.-C. Hon, R. Cao, Y.-C. Liang, Y.-J. Zhao, R.-H. Wang, J.-B. Weng, Polyhedron 21 (2002) 893.
[28] (a) G.A. Barcley, R.S. Vagg, E.C. Watton, Acta Crystallogr., Sect. B 34 (1978) 1833;
(b) B.N. Figgis, E.S. Kucharski, S. Mitra, B.W. Skelton, A.H. White, Aust. J. Chem 43 (1990) 1269.
[29] S.A. Cotton, V. Franckevicius, J. Fawcett, Polyhedron 21 (2002) 2055.
[30] (a) J. Carranza, J. Sletten, F. Lloret, M. Julve, Inorg. Chim. Acta 357 (2004) 3304;
(b) S.R. Marshall, A.L. Rheingold, L.N. Dawe, W.W. Shum, C. Kitamura, J.S. Miller, Inorg. Chem. 41 (2002) 3599.
[31] K. Nakamoto, Infrared and Raman Spectra of Inorganic and Coordination Compounds, Wiley, New York, 1997.
[32] (a) X.-Y. Xu, Q.-H. Luo, M.-C. Shen, X.-Y. Huang, Q.-J. Wu, Polyhedron 16 (1997) 915;
(b) H. Keypour, S. Salehzadeh, R.G. Pritchard, R.V. Parish, Polyhedron 19 (2000) 1633.
[33] A.B.P. Lever, Inorganic Electronic Spectroscopy, 2nd ed., Elsevier Science, Amsterdam, 1984.